Shear Design of RC Members Strengthened with Steel Reinforcing Bars Embedded Through Section

Fiset, M. [(a)], Bastien, J. [(b)], Mitchell, D.[(c)]

(a) Assistant Professor – Université du Québec à Chicoutimi, Department of applied sciences, Saguenay (QC), G7H 2B1, Canada, Mathieu_fiset@uqac.ca (Corresponding author)

(b) Professor – Université Laval, Département de génie civil et de génie des eaux, Québec (QC), G1V 0A6, Canada, Josee.bastien@gci.ulaval.ca

(c) Professor –McGill University, Department of Civil Engineering, Montreal (QC), H3A 0C3, Canada, Denis.mitchell@mcgill.ca

ABSTRACT

The shear strengthening technique investigated in this paper consists of inserting steel reinforcing bars into holes drilled into a shear-deficient existing concrete member and bonding these bars to the concrete with high-strength epoxy adhesive. It is important to realize that current shear design methods are applicable to RC members with conventional stirrups and hence overestimate the shear capacity of members with epoxy-bonded bars. In order to overcome this difficulty, a shear design method for RC members strengthened with epoxy-bonded shear reinforcement is presented. The proposed method was developed considering the development of epoxy-bonded bars as well as the effect of crack width and aggregate interlock on shear capacity. The predicted shear capacities were compared with beam test results and provide accurate predictions.

Keywords: Shear design, shear strength, steel bars embedded-through-section, analytical modelling, bond characteristics, shear strengthening, reinforced concrete.

1 INTRODUCTION

In North America, many reinforced concrete (RC) bridges were built during the ’60s and the ’70s, with thick concrete slabs being a widely used structural system. These structures consist of structural slabs, typically thicker than 500 mm without stirrups. However during the ’90s, it was demonstrated that the maximum concrete shear stress of members without stirrups decreases when increasing member depth over 300 mm [1, 2]. In addition, material degradation as well as an increase of traffic loads may affect the adequacy of these aging bridges in resisting shear.

Most of the shear strengthening techniques studied in the literature, such as Near-Surface Mounted bars (NSM) and Externally Bonded (EB) fabrics, plates and laminates, consist of installing shear reinforcement on the lateral faces of a member [3-23]. These techniques are effective in increasing the shear capacity of beams but are much less efficient for wide structural element applications, such as slabs. The embedment-through-section (ETS) technique illustrated in Fig. 1a consists of inserting reinforcing bars into pre-drilled holes and anchoring the bars to the concrete with high-strength epoxy adhesive [22-34]. Fig. 1b illustrates a member shear strengthened with different configurations of reinforcing bars embedded through the section. As illustrated, additional anchorage may be provided to the epoxy-bonded bar with a steel plate at the bar extremity and bearing on the member surface. Shear reinforcement may also be vertical or inclined with respect to the longitudinal member axis.

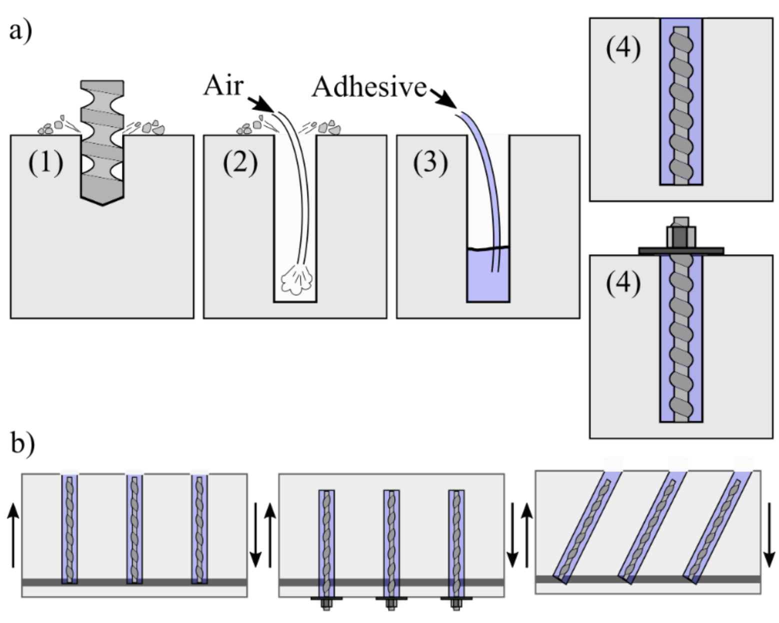

Fig. 1 – a) The installation steps of reinforcing bars embedded through section: (1) drilling of hole, (2) cleaning the hole, (3) injection of high-strength epoxy adhesive and (4) insertion of the reinforcing bar; b) examples of vertical and inclined bonded shear reinforcement configurations, with and without an anchor plate

By testing beams strengthened in shear with epoxy-bonded steel bars embedded through the section, several authors have demonstrated the efficiency of this technique [26-33]. Barros and Dalfré [31] tested 300 mm deep beams with steel bars embedded through the full section depth and showed that the performance of ETS steel bars can be very similar to stirrups. Bédard [26], Cusson [27] and Provencher [28] used steel bars embedded through about 80% of the depths of the beams, which had depths varying from 450 mm to 750 mm, to strengthen thick beams. The shear capacities with steel ETS were increased up to 111% compared with beams without shear reinforcement. The authors observed some debonding of the embedded steel bars and their shear contribution was lower than that for traditional stirrups. The authors showed that the use of design equations from existing codes [35-38], developed for members with properly anchored conventional stirrups, results in an overestimation of the shear capacity of beams with epoxy-anchored bars, as much as 48%. When used in members already containing stirrups, ETS steel bars can also significantly increase the shear capacity, but their performance decreases with the increase of the stirrups amount [31, 32]. A similar effect was noted by several authors studying beams shear strengthened with EB and NSM techniques as well as with ETS FRP bars [23, 39-41]. Current models [24, 34, 42] for predicting the contribution of ETS bars are discussed. A new model is developed in this paper based on the Modified Compression Field Theory [43] that accounts for the bond characteristics of the embedded steel bars and applies to members with and without stirrups.

2 RESEARCH SIGNIFICANCE

Although the shear strengthening technique of RC members with steel reinforcing bars embedded through the section increases shear capacity, the utilisation of current design methods, specified for members with conventional shear reinforcement (stirrups), often leads to an overestimation of the shear capacity of such epoxy-bonded strengthened members. Therefore, current design methods for the shear capacity of members with embedded-through-section steel reinforcing bars need to be adjusted to accurately predict the effect of this type of reinforcement. A design approach is developed that accounts for the bond characteristics of steel bars embedded through the section by considering the influence of crack width and aggregate interlock on the behavior.

3 THEORETICAL BACKGROUND

3.1 Shear capacity of members

Most of the methods specified by international codes (CSA A23.3, CSA S6, AASHTO LRFD, *fib* model code) [35-38] to determine shear capacity of RC members are based on the Modified Compression Field Theory (MCFT) [43]. It is noted that the design equations in CSA S6 are based on the MCFT with a simplification developed by Bentz and Collins [43-45]. The nominal shear capacity of a member, V_n, (material resistance taken as 1.0) is determined from the concrete shear contribution, V_c, and the transverse reinforcement shear contribution, V_s, as follows:

$$V_n = V_c + V_s \tag{1}$$

$$V_c = \beta \sqrt{f_c'}\, b_w d_v \tag{2}$$

$$V_s = A_v f_y \frac{d_v}{s}\left(\cot\theta + \cot\alpha\right)\sin\alpha \tag{3}$$

In these equations, f_c' is the concrete compressive strength, b_w is the width of the web and d_v is the effective shear depth (the greater of $0.9d$ or $0.72h$), h the member depth and d the effective depth measured to the main tension reinforcement. In Eq. (3), s is the stirrup spacing, A_v is the area of transverse reinforcing bars within a distance s, f_y is the yield strength of shear reinforcement, α is the angle between the inclined shear reinforcement and the longitudinal axis of the member and θ is the angle of inclination of the diagonal compressive stresses to the longitudinal member axis. For members with shear reinforcement, the angle, θ, is determined to allow stirrup yielding before concrete crushing in diagonal compression [45] as follows:

$$\theta = 29^\circ + 7000\varepsilon_x \quad (4)$$

Where the longitudinal strain at mid depth, ε_x, can be determined with Eq. (5).

$$\varepsilon_x = \frac{M_u/d_v + 0.5V_u \cot\theta + 0.5N_u - A_p f_{po}}{2\left(E_s A_s + E_p A_p\right)} \quad (5)$$

Where M_u, V_u and N_u are respectively the bending moment, the shear and the axial force (positive in tension) at the section, A_p and A_s are the area of prestressed and non-prestressed longitudinal tension reinforcement, respectively, E_p and E_s are the Young's moduli and f_{po} is the stress in prestressed reinforcement. To consider tensile stress in the diagonally cracked concrete and aggregate interlock at crack interfaces, Collins *et al.* [44] proposed determining β directly from principal tensile strain, ε_1, and average crack width, w, from Eq. (6) in SI units.

$$\beta = \frac{0.33\cot\theta}{1+\sqrt{500\varepsilon_1}} \le \frac{0.18}{0.31+\dfrac{24w}{16+a_g}} \tag{6}$$

Using Eq. (6) resulted in an iterative method not suitable for design purpose. Typically at shear failure, the concrete shear capacity is limited by aggregate interlock (right hand side of Eq. (6)) at the crack interfaces. Codes [35-38] adopted the following simplified equation proposed by Bentz and Collins [45] to determine β in SI units.

$$\beta = \left(\frac{0.4}{1+1500\varepsilon_x}\right)\left(\frac{1300}{1000+s_{ze}}\right) \tag{7}$$

The crack spacing parameter s_{ze} is taken as 300 mm for members containing minimum shear reinforcement and respecting the maximum spacing requirements for the stirrups. For members without shear reinforcement, s_{ze} is taken as $k_{dg}d_v$, where $k_{dg} = 35/(15+a_g) \geq 0.85$. Comparing Eq. (6) and (7), the average crack width at shear failure of a member with shear reinforcement may be estimated from Eq. (8) in mm unit for members with shear reinforcement [45].

$$w = 0.2 + 1000\varepsilon_x \tag{8}$$

3.2 Behavior of bonded bars

The previously presented shear design method was developed for stirrups. To consider the bond behavior of bonded shear reinforcement in shear design, the pull-out response of bonded bars embedded in concrete was investigated by many authors [46-54]. The typical bond-slip response of epoxy-bonded bars is presented in Fig. 2a, where s_1 and s_2 are the slips at the peak bond stress, and f_{b0} is the basic bond strength of the adhesive given by the manufacturer. Typically for properly installed bonded bars, s_1 = 0.8 to 1 mm, s_2 = 2 mm [52-55]. To consider concrete breakout, the bond strength, f_b, is limited as expressed by the following equation [53-55].

$$f_b = f_{b0} \leq \frac{k_c \Omega_\theta}{\pi d_b}\sqrt{f'_c \ell} \tag{9}$$

$$\Omega_\theta = 0.30 + \tanh\left(\frac{10}{\theta + \alpha - 115°}\right) \leq 1 \tag{10}$$

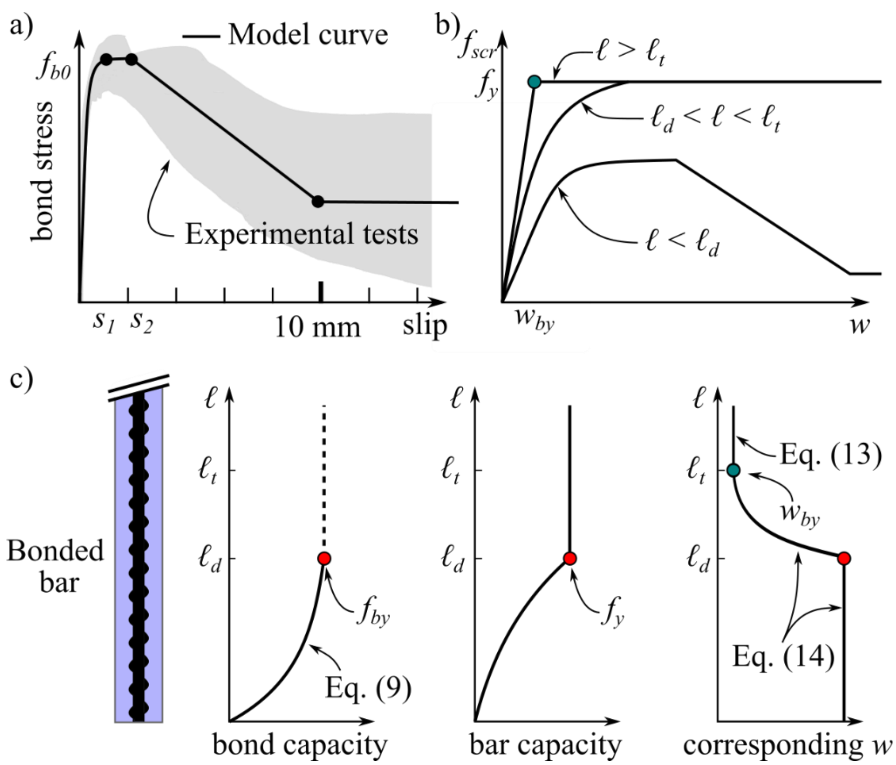

Fig. 2 – a) Bond vs slip relationship and comparison to tests carried out by Villemure *et al.* [50] ($2\,d_b \leq \ell \leq 4\,d_b$), b) axial bar stress at a crack according to the crack width and c), maximum value of bond stress, corresponding maximum axial bar stress and corresponding crack width as a function of the embedment length, ℓ

Where ℓ is the embedded length and k_c is the concrete capacity factor defined by the codes and the adhesive manufacturer [36, 56, 57]. Typically, the average k_c = 14.7 and k_c = 7.0 with a 5% fractile, in SI units. The factor, Ω_θ, determined with Eq. (10) accounts for the reduction of the concrete breakout capacity for inclined bars crossed by diagonal cracks [55]. Considering that a steel plate can be used at a bar extremity to increase anchorage [58, 59], the development length, ℓ_d, of a bonded bar can be determined from Eq. (11), where f_{by} is the uniform bond strength at yielding of the bar given by Eq. (12) and d_a is the diameter of the anchorage plate if present, d_a = 0 otherwise

$$\ell_d = \left(\frac{f_y d_b}{4 f_{by}}\right)\left(\frac{1}{1+0.667\left(d_a / \ell_d\right)}\right)^{2/3} \tag{11}$$

$$f_{by} = \sqrt[3]{\frac{\Omega_\theta{}^2 k_c{}^2 f_c' f_y}{40 d_b}} \leq f_{b0} \tag{12}$$

<u>3.3 Bonded bar response at a shear crack</u>

Before yielding of a bonded bar, the axial bar stress at a crack, f_{scr}, is a function of the available bar embedded length defined by the crack location and the crack width, w. As shown in Fig. 2b and in Fig. 2c, bonded bars may experience three typical types of behavior depending on the location of the crack [53]. For a crack located such that there is an embedded length, ℓ, longer than the transition length, ℓ_t, yielding of the bar occurs for a thin crack, w_{by}, and the bonded bar stress at the crack can be determined from Eq. (13). For a crack located such that there is a shorter embedment length, $\ell \leq \ell_t$, bar pullout ($\ell < \ell_d$) or bar yielding ($\ell_d \leq \ell \leq \ell_t$) can occur for a large crack (Fig. 2c), and the axial bar stress at a crack can be determined from Eq. (14).

$$\text{if } \ell > \ell_t \quad f_{scr} = \frac{w}{w_{by}} f_y \leq f_y \tag{13}$$

$$\text{if } \ell \leq \ell_t \quad f_{scr} = \frac{4 f_b \ell k_d}{d_b} \sqrt{1 - \exp\left(\frac{k_w \left(f_{scr} w_{by} - 2 f_y w \right)}{2\alpha_0 f_y} \right)} \leq f_y \tag{14}$$

In the previous equations, k_w is the ratio between the bar displacement at a crack and the crack width given by Eq. (15), which can safely be taken as 0.9 for vertical bars and 0.6 for bars inclined at 45°.

$$k_w = 0.75 \sin\left(\theta + \alpha\right) - 0.5 \cos\left(\theta + \alpha\right) \tag{15}$$

In this equation, α is the angle between the bars and the longitudinal member axis. The debonding factor, k_d, the crack width at yielding, w_{by}, and the transition length, ℓ_t, of the bonded bar may be determined from Eqs. (16) through (18) [51].

$$k_d = 1 - \frac{k_w w - s_2}{d_b} \begin{cases} \geq 0.4 \\ \leq 1.0 \end{cases} \tag{16}$$

$$w_{by} = \frac{f_y}{k_w} \sqrt{\frac{d_b}{k_0 E_s}} \tag{17}$$

$$\ell_t \left(\frac{f_{b0}}{\ell_d \; f_{by}} \right) = 0.8 + 0.8 \left(\frac{\alpha_0}{k_w w_{by}} \right)^{0.7} \geq 1 \tag{18}$$

In these equations, k_0 and α_0 are two parameters defining the bond-slip curve. k_0 can be estimated as $2.5 f_{b0} / s_1 \approx 40$ to 80 MPa/mm and $\alpha_0 \approx 0.45$ mm for typical deformed rebars [53, 60].

4 MEMBER RESPONSE

Fig. 3 presents a bonded bar intersected by a shear crack. For this bonded bar, the bar embedment, ℓ, is defined by the crack location, x_{cr}, so that the bonded bar stress and the corresponding crack width can be determined from Eqs. (13) or Eq. (14) (see Fig. 2b) and plotted in Fig. 3. For comparison purposes, the response of a stirrup determined with the model proposed by Fernández Ruiz *et al.* [61] is also presented.

Three zones may be identified (ZS, ZT and ZD) along the shear depth based on the typical behavior exhibited by the bonded bar at the crack (Fig. 2b). If the crack intercepts a bonded bar far from its extremities in a zone ZS ($\ell > \ell_t$), the bonded bar response is similar to a cast-in-place stirrup and a thin crack leads to the bar yielding. For an intermediate embedment in a zone ZT ($\ell_d \leq \ell < \ell_t$), to develop yielding a larger crack is required for a bonded bar than for a stirrup. The effect of this zone is however limited to a small portion of the member since debonding may limit the bonded bar capacity for a shallower embedment ($\ell < \ell_d$) in the zone ZD. For comparison, the response of stirrups is not affected by the bar embedment depth due to the anchorage performance and all stirrups may reach yielding in the presence of thin cracks [61-64].

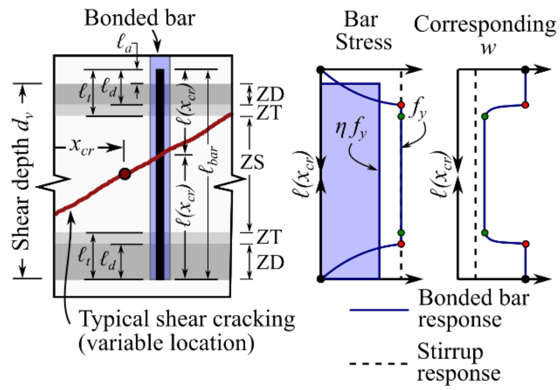

Fig. 3- Development of a bonded bar stress and corresponding crack width, and comparison to a stirrup.

In a member with shear reinforcement, the bar stress and the shear crack width affect the shear resistance mechanisms. Fig. 4 presents the response and the shear resistance mechanisms in a cracked reinforced concrete member with bonded shear reinforcement according to the critical shear crack width. The total shear transmitted by shear reinforcement, V_s, corresponds to the force carried by every bonded bar intercepted by the diagonal shear crack, while the concrete shear capacity is determined from Eq. (2).

As presented in Fig. 4 for a case with two bonded bars intercepted by a diagonal shear crack, the crack opening activates the bars. When all the bonded bars are intercepted in the zone ZS ($\ell > \ell_t$ for all bars in Fig. 4a), the bonded bars response is similar to cast-in-place stirrups. A small crack opening leads to the yielding of all bonded bars and the shear capacity V_s is similar to stirrups. Also, the difference between the crack widths corresponding to that V_s for a member with bonded bars and a member with stirrups, Δ_w, is small.

When a bonded bar is intercepted in a zone ZT ($\ell_d \le \ell < \ell_t$ for one bar in Fig. 4b), the crack has to open more to enable yielding of that bonded bar. By comparing to the response of a member with stirrups, similar V_s is expected but difference between the corresponding crack widths, Δ_w, is larger.

When a bonded bar is intercepted in a zone ZD ($\ell < \ell_d$ for one bar in Fig. 4c), debonding may occur and limit the bonded bar shear capacity. In that case, the bonded bar shear capacity, V_s, is lower than the capacity provided by stirrups. Also, the corresponding crack width is larger for a member with bonded bars than a member with stirrups, and the difference between crack widths, Δ_w, can be important in that zone.

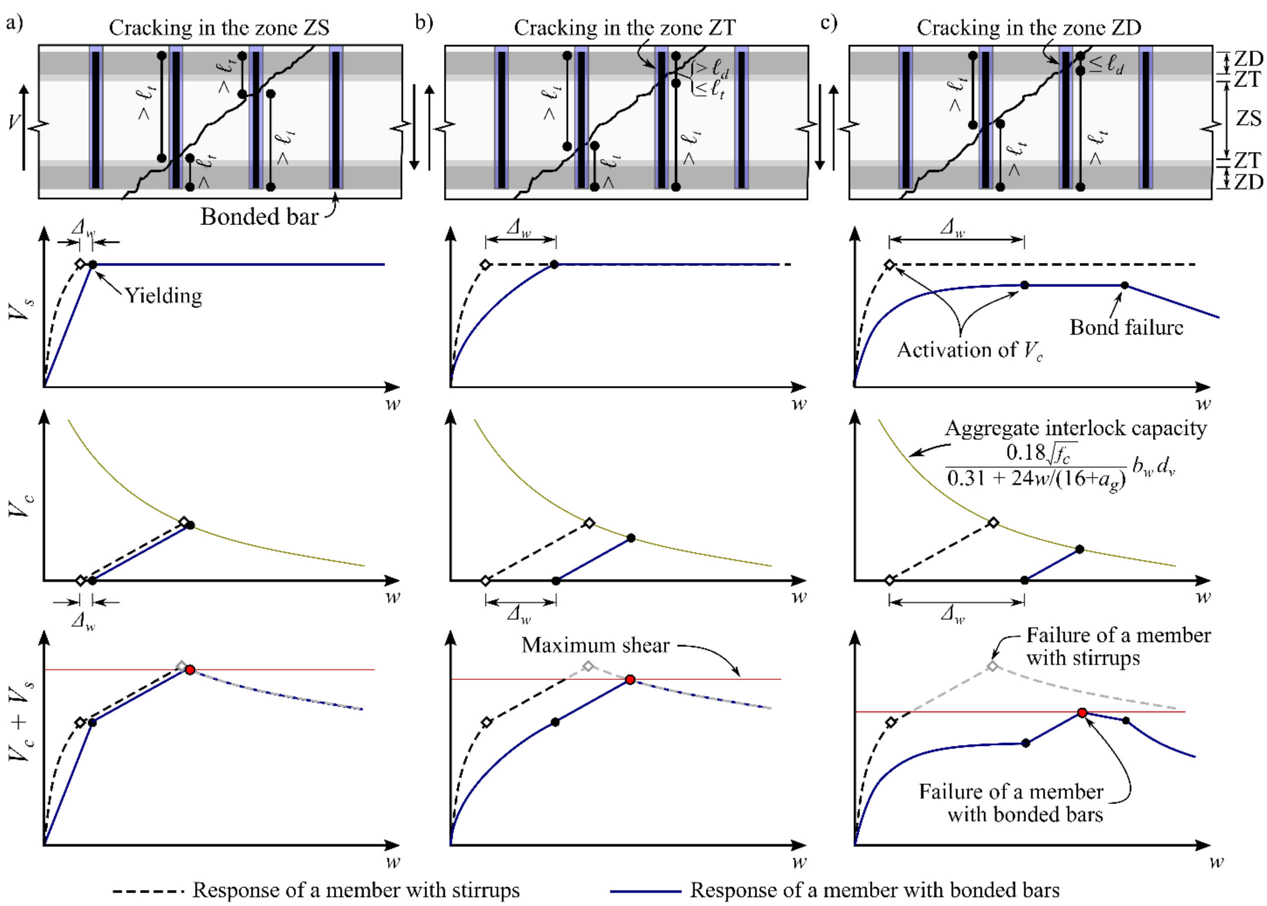

Fig. 4- Shear response of a member with bonded bars according to the critical shear crack width intercepting a bar in the zones a) ZS, b) ZT, and c) ZD

After the shear reinforcement reaches its maximum capacity, further increase in shear requires the activation of aggregate interlock ($V_c > 0$) [2, 43-45, 65]. That activation is mainly influenced by the amount of flexural reinforcement, the applied shear and the crack orientation [66]. For a given crack location, similar beams with different types of shear reinforcement (bonded or stirrups) present parallel curves V_c versus w and the difference in crack widths remains approximatively constant until shear failure occurs. This cracking behavior was experimentally observed by Fiset *et al.* [55]. Since a member with bonded bars may experience larger crack widths compared to a similar member with stirrups (Fig. 4), the resulting reduced aggregate interlock leads to a reduced concrete shear contribution, V_c.

5 PROPOSED DESIGN METHOD

5.1 Shear contribution of steel reinforcing bars embedded through section (ETS)

The proposed design method considers that a RC member loaded in shear typically contains many diagonal cracks randomly distributed in the web to determine the average shear capacity. This random cracking results in a distributed bonded bar contribution and corresponding crack widths as illustrated in Fig. 2 to Fig. 4. Within the shear depth, the average bonded bar axial capacity is illustrated by the shaded area in Fig. 3 and is lower than the bar yield stress due to the development of the bonded bar and the behavior presented in Fig. 4. This average stress is given by ηf_y, with η characterizing the bonded bar efficiency.

The efficiency factor, η, may be determined by integrating the axial bar capacity given by Eqs. (13) or (14) in the zones ZS, ZT and ZD. Typically, in the zone ZS, yielding of a bonded bar occurs for a thin crack width similar to the response for a stirrup (refer to Eqs. (17) and (25)). Since the angle θ in Eq. (4) is selected to enable stirrup yielding, it can be considered that bonded bars develop their yield stress within this zone at shear failure. A similar assumption may be considered for the zone ZT since its length is generally limited to a small portion of the member and the bar capacity is generally limited by steel yielding [53]. Within the zone ZD, it can be demonstrated from Eq. (14) that the average bar stress corresponds to 40% of the maximum bonded bar capacity. By considering that a bonded bar may exceed the shear depth (see Fig. 3) to reduce the effect of the zone ZD, η can be determined from Eq. (19).

$$\eta = \frac{\ell_{bar}\sin\alpha}{d_v} - \frac{\Sigma\ell_d \sin\alpha}{d_v}\left(1-0.4k_d\left(1-\left(\frac{\Sigma\ell_a}{\Sigma\ell_d}\right)^{2.5}\right)\sqrt{1-\exp\left(\frac{k_w}{\alpha_0}\left(0.2w_{by}-w\right)\right)}\right)\leq 1 \tag{19}$$

Where w is the average shear crack width, ℓ_{bar} is the length of the bonded bar, $\Sigma\ell_d$ refers to the summation of ℓ_d determined at both the bonded bar extremities (Eq. (11)) and $\Sigma\ell_a$ is the total length of the bar exceeding the shear depth (see Fig. 3) contributing to the anchorage and determined from Eq. (20).

$$\Sigma\ell_a = \ell_{bar} - \frac{d_v}{\sin\alpha}\begin{cases}\geq 0\\ \leq \Sigma\ell_d\end{cases} \tag{20}$$

Considering Eq. (8), the average shear crack width at shear failure for a member with bonded shear reinforcement may be estimated from Eq. (21) in mm unit.

$$w = 0.2 + 1000\varepsilon_x + \Delta_w \tag{21}$$

Where Δ_w is the difference between the average crack width for a member with bonded bars and a member with stirrups (see Fig. 4). From Eq. (3) and considering the average bonded bar capacity, ηf_y, the average shear contribution provided by the bonded shear reinforcement can be determined as follows:

$$V_s = \eta f_y A_v \frac{d_v}{s}\left(\cot\theta + \cot\alpha\right)\sin\alpha \tag{22}$$

5.1.1 Simplification for design

Typically, RC members with shear reinforcement exhibit large diagonal cracks at shear failure, thus the maximum bond is reached within the zone ZD [26-30]. In that case, the square root term in Eq. (19) is close to 1 and the bond efficiency factor, η, can be determined with Eq. (23).

$$\eta = \frac{\ell_{bar} - \Sigma\ell_d\left(1 - 0.4k_d\left(1 - \left(\Sigma\ell_a / \Sigma\ell_d\right)^{2.5}\right)\right)}{d_v / \sin\alpha} \le 1 \tag{23}$$

Fig. 5 compares the average bond efficiency factor η determined from Eqs. (19) and (23) for a typical RC member with different types of bonded shear reinforcement. It can be observed that for a crack width larger than about 0.7 mm, the difference between Eq. (19) and (23) is very small (less than 4%), and this difference decreases for a larger crack. Also, it can be seen that the steel yield stress has a very little effect on η determined with Eq. (19).

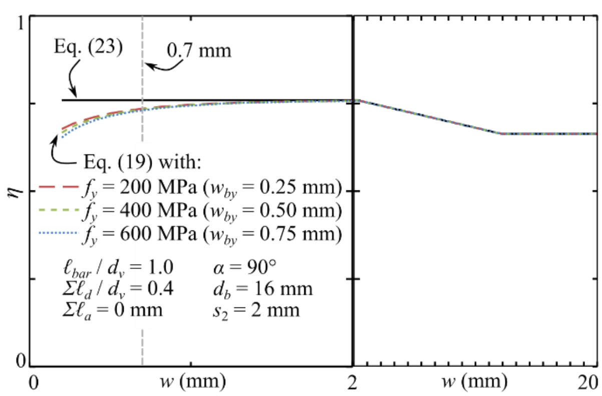

Fig. 5 – Bonded reinforcement efficiency factor determined with Eqs. (19) and (23) according to the critical shear crack width for a typical RC member

5.2 Shear contribution of concrete

Referring to Fig. 4, the difference in average crack widths, Δ_w, affecting the shear contribution of concrete, V_c, can be determined for a specific shear crack location, x_{cr}, depending on the intercepted zones ZD, ZT and ZS. Considering that the shear crack location is variable, the distribution of Δ_w can be determined along the member as illustrated in Fig. 6 for the case of a shear crack intersecting two bonded bars. This distribution follows a repeating pattern characterized by three typical values of Δ_w associated with the three cases illustrated in Fig. 4 and the zones ZD, ZT and ZS activated by the shear crack.

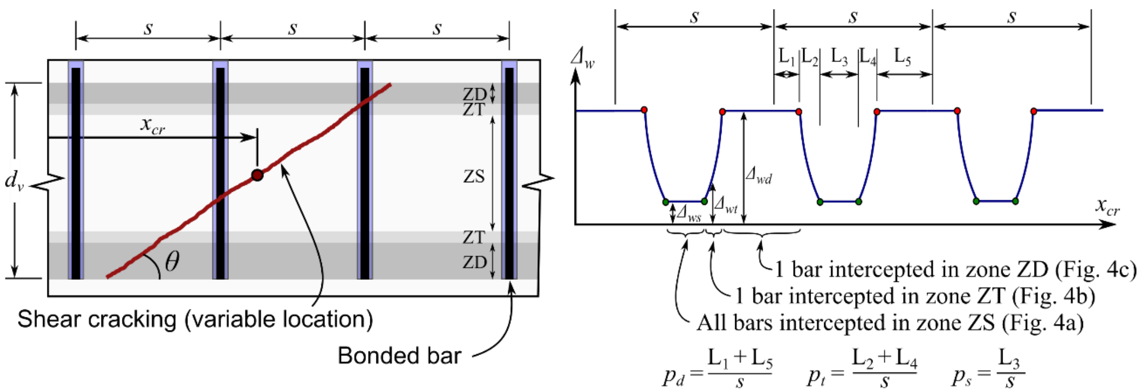

Fig. 6 – Difference between the crack widths, Δ_w, corresponding to V_s according to the shear crack location determined along the member (refer to Fig. 4)

For the bonded bars being intercepted in the zone ZS, the shear reinforcement yields and the difference in average crack width, Δ_{ws} can be determined as follows:

$$\Delta_{ws} = w_{by} - w_{sy} \tag{24}$$

Where w_{by} and w_{sy} are the crack width at yielding of a bonded bar (Eq. (17)) and a stirrup, that can be determined from the Fernández Ruiz *et al.* [61] model as follows:

$$w_{sy} = \frac{d_b f_y^{\,2}}{2.5 k_w E_s f_c'^{\,2/3}} \quad (25)$$

Eq. (25) is similar to the one proposed by Fernández Ruiz *et al.* [25] and considers the orientation of the crack with the parameter k_w [51] and a bond strength between a steel bar and the surrounding concrete of $0.6\, f_c'^{\,2/3}$ [61, 67]. For the case with at least one bonded bar being intercepted in zone ZD, the average bonded bar displacement at a crack prior to debonding corresponds to the slip s_1 and half of w_{by} determined for an average axial stress of 0.4 f_y increased by the effect of the anchorage length ℓ_a. The difference in crack width, Δ_{wd}, can be simplified from Eqs. (13), (14) and (25) as follows:

$$\Delta_{wd} = \frac{s_1}{k_w} + 0.2 w_{by} \left(\frac{\Sigma\ell_d}{\Sigma\ell_d - \Sigma\ell_a} \right) \left(1 - \left(\frac{\Sigma\ell_a}{\Sigma\ell_d} \right)^{2.5} \right) - w_{sy} \quad (26)$$

Otherwise, the average difference in crack width is given by the behaviour of a bonded bar in the zone ZT, Δ_{wt}. Considering the yielding of the bonded bar, Δ_{wt} can be determined from the simplification of Eqs. (14) and (25) as follows:

$$\Delta_{wt} = \frac{\alpha_0}{4k_w} \left(\frac{\Sigma\ell_d}{\Sigma\ell_t - \Sigma\ell_d} \right) \left(\frac{f_{by}}{f_{b0}} \right) + 0.5\Delta_{ws} \quad (27)$$

More details about the development of Eqs. (26) and (27) can be found in Fiset [51] and Fiset *et al.* [53]. When an anchorage plate is used at a bar extremity, the difference in crack width at that extremity may be considered negligible [62, 63]. Considering that a RC member loaded in shear typically contains many diagonal cracks randomly distributed, V_c can be determined from an average value of Δ_w given as follows:

$$\Delta_w = p_d \Delta_{wd} + p_t \Delta_{wt} + p_s \Delta_{ws} \geq 0 \tag{28}$$

In Eq. (28), p_d, p_t and p_s are the proportion of the member affected by Δ_{wd}, Δ_{wt} and Δ_{ws}, respectively. These proportions may be estimated graphically as illustrated in Fig. 6. Considering the average increase in crack width, Δ_w, given in Eq. (28) for partially developed bonded bars results in an increased crack width, w, given in Eq. (21). Then, substituting Eq. (21) into the aggregate interlock expression in the right hand side of Eq. (6), the expression for β accounts for the increase in crack width, Δ_w. The resulting expression for β developed by Bentz and Collins [45] to determine concrete shear capacity can then be adjusted as follows:

$$\beta = \left(\frac{0.4}{1 + 1500\varepsilon_x + 1.5 k_{dg} \Delta_w} \right) \left(\frac{1300}{1000 + s_{ze}} \right) \tag{29}$$

5.2.1 Simplification for design

Typically, the effect of the zones ZT and ZS are limited since p_t, Δ_{wt} and Δ_{ws} values are small. For design, the effect of these two zones may be neglected and Eq. (28) safely can be simplified as follows (mm and MPa units):

$$\Delta_w = \frac{p_d}{k_w} \left[s_1 + 0.05 \left(1 + 1.5 \frac{\Sigma \ell_a}{\Sigma \ell_d} \right) \left(\frac{f_y}{400} \sqrt{\frac{d_b}{3}} \right) - \frac{1}{{f_c'}^{2/3}} \left(\frac{f_y}{400} \sqrt{\frac{d_b}{3}} \right)^2 \right] \geq 0 \tag{30}$$

The proportion p_d can then be conservatively estimated from Eq. (31), where n_p is the number of extremities of a bonded bar with an anchorage plate.

$$p_d = \left(\frac{2-n_p}{2}\right)\left(\frac{\Sigma\ell_d - \Sigma\ell_a}{s}\right)\sin\alpha\left(\cot\theta + \cot\alpha\right)\begin{cases}\leq 1\\ \geq 0\end{cases} \tag{31}$$

Fig. 7 compares Δ_w determined from Eq. (28) and Eq. (30). In the case of p_d = 1 in Fig. 7a and b, it can be seen that Eq. (30) provides a good approximation for the effects of d_b, $\Sigma\ell_a/\Sigma\ell_d$, f_y and f_c'.

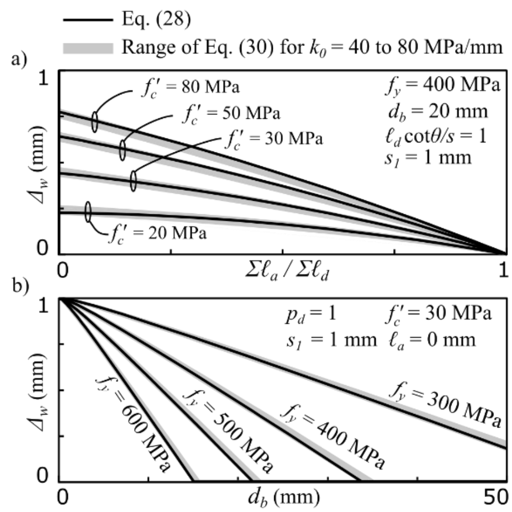

Fig. 7 - Comparison between Δ_w determined from Eq. (28) and Eq. (30) as a function of a) f_c' and $\Sigma\ell_a/\Sigma\ell_d$, and b) f_y and d_b of vertical bonded reinforcing bars

5.3 Maximum spacing and minimum reinforcement

The design codes specify a minimum amount of shear reinforcement and a maximum longitudinal spacing of stirrups [35, 68-70]. The minimum amount of shear reinforcement is provided to prevent a brittle shear failure at first diagonal shear cracking. The maximum longitudinal spacing of stirrups is specified to ensure that a diagonal shear crack intercepts at least 2 consecutive shear reinforcing bars. Members with at least the minimum amount of shear reinforcement and that satisfy the maximum stirrup spacing provide better crack control, a larger shear capacity and some ductility compared to members without shear reinforcement [68-70]. For wide concrete sections and slabs, Lubell *et al.* [71] and Serna-Ros *et al.* [72] also suggested limiting the transverse spacing of shear reinforcing bars, s_w, to the member depth. Considering the average lower bonded bar contribution, these requirements can be expressed as follows:

$$A_v \geq C \frac{\sqrt{f_c'}}{\eta f_y} b_w s \tag{32}$$

$$s \leq \eta \left(k_v + 0.5 \cot \alpha \right) d_v \tag{33}$$

$$s_w \leq \eta d \tag{34}$$

In these equations, C and k_v are parameters defined by codes for stirrups (C = 0.060 and k_v = 0.75 for CSA-S6 [37], C = 0.083 and k_v = 0.80 for AASHTO [38] and C = 0.080 and k_v = 0.83 for fib [35]). The parameters C and k_v were chosen to match those in CSA-S6 because both the proposed design approach and CSA-S6 are based on the MCFT.

5.3.1 Effect of the maximum bar spacing

The effect of the bonded bar spacing is presented in Fig. 8 and Fig. 9. In these figures, the average values corresponding to the proposed design method are compared to the discrete values determined at a crack, considering the bonded bar embedment defined by the crack location, x_{cr}. The value of Δw, and the shear resistance contributions, V_c and V_s, in a member with bonded bars are schematically represented according to x_{cr} in Fig. 8 for three similar members. The members illustrated from Fig. 8 a) to c) contain the same amount of vertical bonded shear reinforcement $A_v / b_w s$ corresponding to the minimum permitted by Eq. (32). The ratio η and the material properties are the same for all members so that it may be expected that the three members have similar average capacities V_c and V_s, and the same shear cracking orientation, θ. However, the longitudinal spacing of the bonded bars, s, increases from Fig. 8 a) to c), with a longitudinal spacing $s = k_v \eta d_v$ corresponding to the maximum permitted by Eq. (33) in Fig. 8b). Therefore, the values at cracks differ along the member due to the bonded bar spacing. The resulting average shear strengths, V_{avg}, are compared in Fig. 9 to the ones determined at cracks, V_{crack}, according to the bonded bar spacing for different angles used to define the maximum spacing.

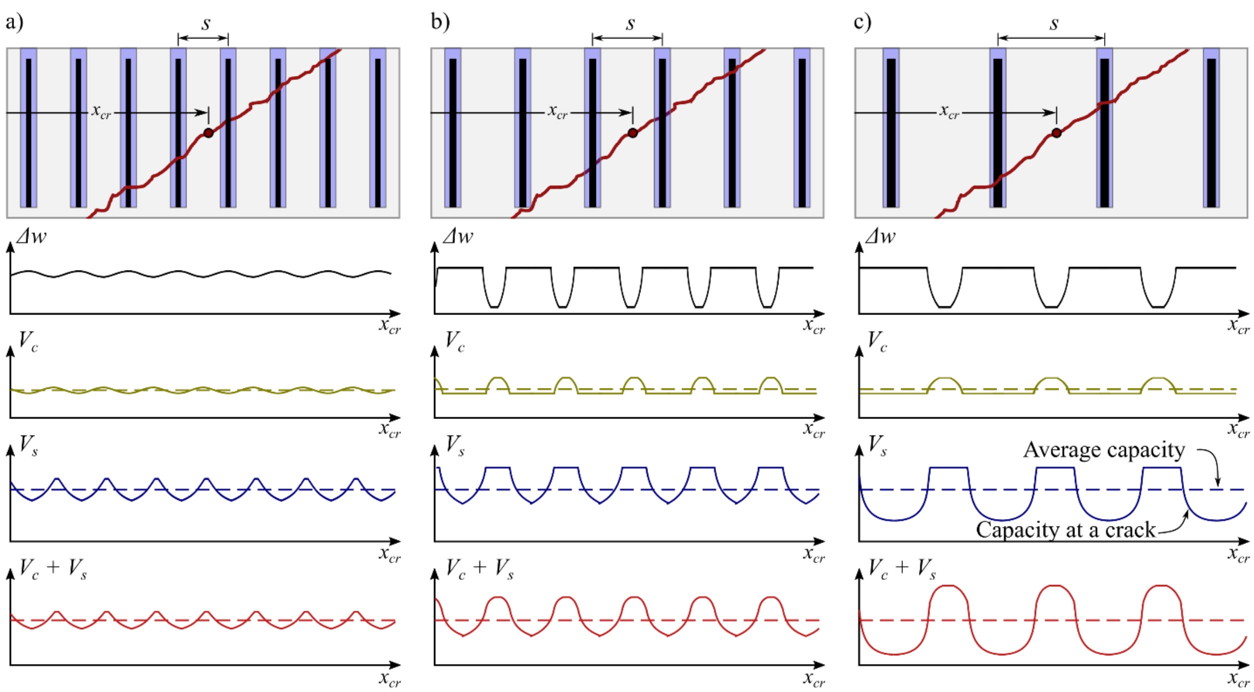

Fig. 8 - Shear strength of similar RC members with a) closely spaced bonded bars, b) bonded bars spaced at the maximum spacing for bonded bars, $\eta k_v d_v$, and c) bonded bars spaced at the maximum spacing for stirrups, $k_v d_v$

When the bar spacing is smaller than the maximum proposed by Eq. (33), it can be seen from Fig. 8a that all cracks inclined at an angle θ intercept a similar number of zones ZD, ZT and ZS. The shear resistance mechanisms V_c and V_s, and the shear capacity determined along the member are very similar to the average values.

When the bar spacing corresponds to the maximum permitted in Fig. 8b, the bonded shear reinforcement capacity is $V_s = 2A_v f_y$ and its distribution along the member is relatively constant. Cracks may intercept different portions of the member so that the difference in crack width, Δ_w, varies more along the member as well as V_c. It can be seen in Fig. 9 that the ratio V_{crack}/V_{avg} is generally between 0.88 and 1.12 when the bonded bar spacing respects the maximum proposed in Eq. (33) ($s/d_v \leq \eta k_v$ for vertical bars). This ratio becomes closer to 1.0 for a smaller spacing.

When the bar spacing is larger than the maximum proposed for bonded bars by Eq. (33), few cracks may develop less than two bonded bars. For the member illustrated in Fig. 8c, the bonded bars spacing corresponds to the maximum spacing for stirrups ($s = k_v d_v$) so that a crack may intercept a bar at its very extremity. For that crack within the zone ZD, one bonded bar is developed ($V_s = A_v f_y$), which corresponds to half the number of bars developed in the member respecting the proposed maximum spacing in (b). Moreover, the development of the bonded bars required a large crack in the zone ZD ($\Delta_{wd} \approx 1$ mm), leading to a V_c at the crack that is smaller than the average value and, also, a lower value of V_s. On the other hand, few cracks may intercept 2 bonded bars within zone ZS resulting in a larger V_c and $V_s = 2A_v f_y$. That explains the large variation of shear strength (ratio V_{crack}/V_{avg} between 0.72 and 1.23) for values of s/d_v between the value of ηk_v (Eq. (33)) and the maximum permitted value of k_v for stirrups as illustrated in Fig. 9.

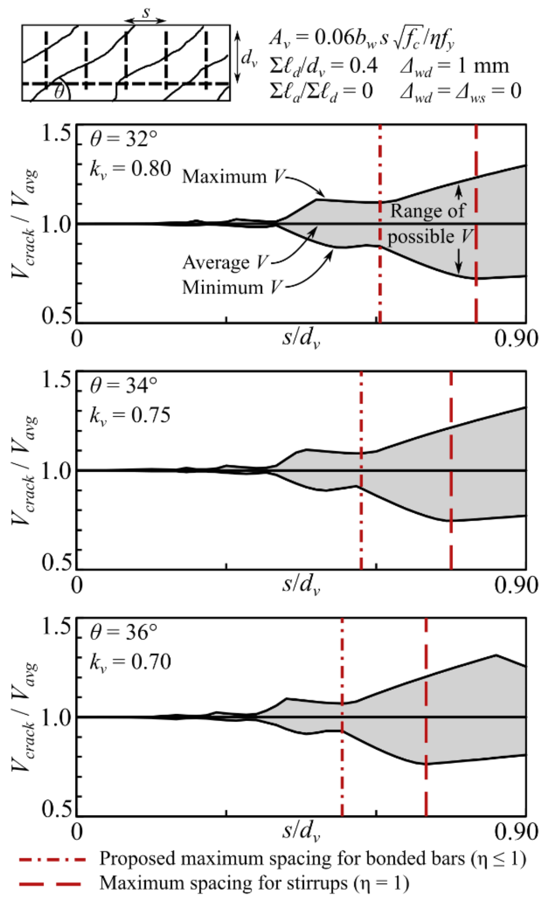

Fig. 9 - Comparison between the average shear strength and the values determined at cracks in a RC member with the minimum amount of vertical reinforcement (α = 90°) according to the bonded bar spacing and the angle used to define the maximum spacing

6 VALIDATION OF THE SHEAR DESIGN METHOD

6.1 Description of test specimens

Table 1 presents the properties of shear critical members strengthened in shear with embedded-through-section (ETS) steel reinforcing bars. Forty-seven beams without stirrups and 10 beams with stirrups were shear strengthened with ETS steel bars. Among these beams, 30 were strengthened with vertical steel ETS (α = 90 degrees) and 27 were strengthened with steel ETS at an angle, α, of 45 degrees. In Table 1, the number of specimens of the same geometry is indicated by n. For those beams with the same geometry, the failure shear, V_{test}, is reported as the average value of the n tests because of the small variation in the results.

Tests	[ref]	n	f'_c	b_w	h	d	ρ_s	ETS bars A_v	ETS bars s	ETS bars α	ETS bars d_b	ETS bars f_y	Stirrups A_v	Stirrups s	Stirrups f_y	V_{test}
			MPa	mm	mm	mm	%	mm²	mm	deg	mm²	MPa	mm²	mm	MPa	kN
1B	[28]	1	33.5	610	450	370	3.10	400	240	90	16.0	480	-	-	-	470
2B	[28]	2	34.9	610	450	398	2.06	200	260	90	11.3	436	-	-	-	301
3B	[28]	2	35.6	610	750	699	1.17	400	470	90	16.0	480	-	-	-	496
#2	[27]	2	34.5	610	750	694	1.65	400	380	90	16.0	448	-	-	-	754
#3	[27]	2	32.6	610	750	694	1.65	800	380	90	16.0	448	-	-	-	878
R375	[26]	4	40.2	610	750	683	2.04	400	375	90	16.0	449	-	-	-	819
R413	[26]	3	39.6	610	750	683	2.04	400	413	90	16.0	449	-	-	-	685
SSB-S6@0.7d	[30]	1	51.9	110	190	150	0.93	28	105	90	6.0	575	-	-	-	42
SSB-S6@d	[30]	1	51.9	110	190	150	0.93	28	150	90	6.0	575	-	-	-	43
SSB-S8@0.7d	[30]	1	51.9	110	190	150	0.93	50	105	90	8.0	530	-	-	-	44
SLB-2S8@d	[30]	1	51.9	450	350	260	1.26	101	245	90	8.0	530	-	-	-	353
H1	[73]	5	32.9	300	410	360	1.31	200	360	45	15.9	547	-	-	-	222
H2	[73]	5	35.6	600	410	360	1.31	200	360	45	15.9	547	-	-	-	371
H3	[73]	5	35.7	900	410	360	1.31	200	360	45	15.9	547	-	-	-	523
H4	[73]	2	31.3	375	410	360	0.79	200	360	45	15.9	547	-	-	-	222
H5	[73]	2	31.3	935	410	360	0.79	200	360	45	15.9	547	-	-	-	405
0S-S300-90	[32]	1	29.7	180	400	360	2.79	79	300	90	10.0	549	-	-	-	131
0S-S300-45	[32]	1	29.7	180	400	360	2.79	79	300	45	10.0	549	-	-	-	209
0S-S180-90	[32]	1	29.7	180	400	360	2.79	79	180	90	10.0	549	-	-	-	154
0S-S180-90	[32]	1	29.7	180	400	360	2.79	79	180	45	10.0	549	-	-	-	221
A3	[31]	1	30.8	150	300	262	2.50	79	300	90	10.0	542	-	-	-	96
A4	[31]	1	28.8	150	300	262	2.50	79	300	45	10.0	542	-	-	-	122
B3	[31]	1	30.8	300	300	262	1.88	101	300	90	8.0	567	-	-	-	144
B4	[31]	1	28.8	300	300	262	1.88	101	300	45	8.0	567	-	-	-	202
2S-S300-90	[32]	1	29.7	180	400	360	2.79	79	300	90	10.0	549	57	300	574	189
2S-S300-45	[32]	1	29.7	180	400	360	2.79	79	300	45	10.0	549	57	300	574	244
2S-S180-90	[32]	1	29.7	180	400	360	2.79	79	180	90	10.0	549	57	300	574	244
2S-S180-45	[32]	1	29.7	180	400	360	2.79	79	180	45	10.0	549	57	300	574	303
4S-S300-90	[32]	1	32.3	180	400	360	2.79	79	300	90	10.0	549	57	180	574	223
4S-S300-45	[32]	1	32.3	180	400	360	2.79	79	300	45	10.0	549	57	180	574	332
4S-S180-90	[32]	1	32.3	180	400	360	2.79	79	180	90	10.0	549	57	180	574	248
4S-S180-45	[32]	1	32.3	180	400	360	2.79	79	180	45	10.0	549	57	180	574	340
A5	[31]	1	30.8	150	300	262	2.50	79	300	90	10.0	542	57	300	559	139
B5	[31]	1	30.8	300	300	262	1.88	101	300	90	8.0	567	57	300	559	234

Note: f_c' taken as 85% of the compressive strength measured on cubes [35]

Table 1 – Summary of properties and shear strengths of members with ETS steel bars

6.2 Comparison of predictions with experimental results

Fig. 10 compares the predicted capacities with the shear strengths, V_{test}. Fig. 10a compares the nominal capacities, V_{csa}, determined with Eq. (1) to (7) for members assuming that the shear reinforcement consists of conventional stirrups (η = 1, Δ_w = 0). Fig. 10b and c compare the strength predictions using the detailed method, V_{det}, and the simplified method, V_{sim}, with the values of V_{test}. For the case of ETS steel bars and stirrups, the additional strength provided by ETS bars (Eq. (22) is added to the V_s term in Eq. (3).

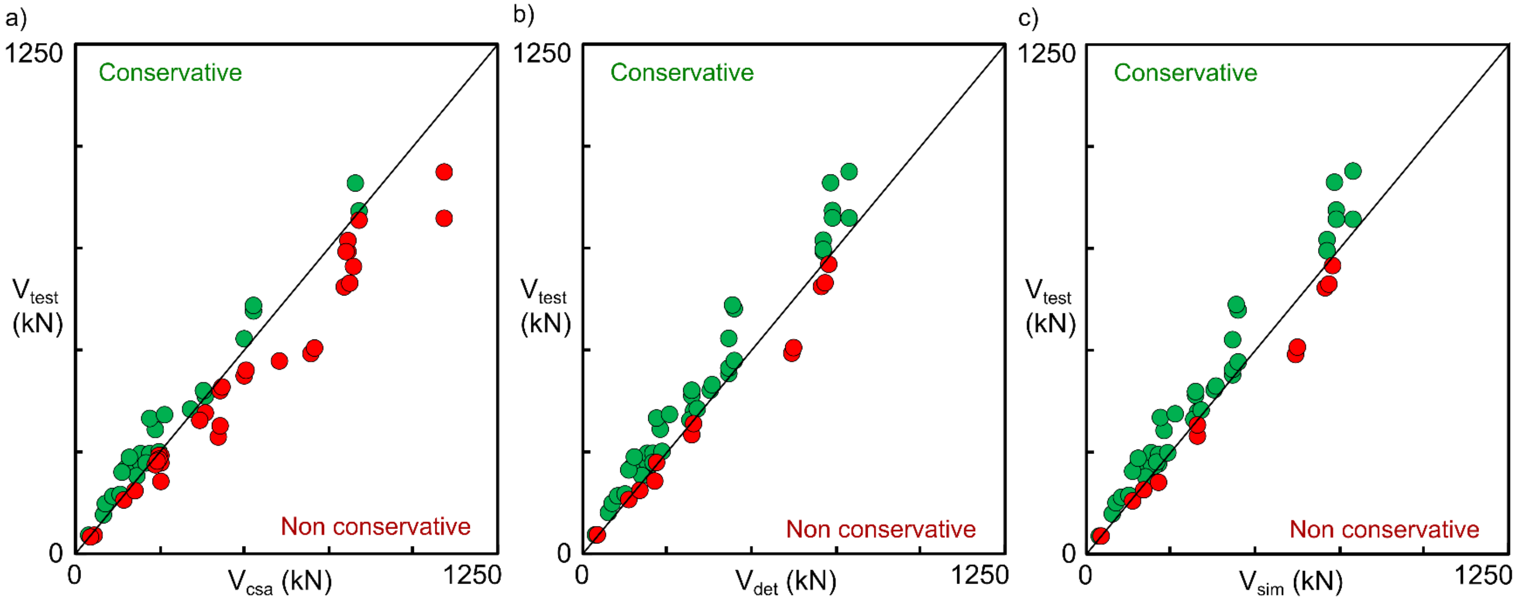

V_{test}/V_{csa}		with stirrups	without stirrups	total
90° ETS	n	6	24	30
	avg	1.15	0.89	0.94
	CoV	16%	15%	19%
45° ETS	n	4	23	27
	avg	1.33	1.01	1.06
	CoV	8%	18%	19%
total	n	10	47	57
	avg	1.22	0.95	1.00
	CoV	14%	18%	20%

V_{test}/V_{det}		with stirrups	without stirrups	total
90° ETS	n	6	24	30
	avg	1.19	1.00	1.04
	CoV	15%	12%	14%
45° ETS	n	4	23	27
	avg	1.33	1.10	1.14
	CoV	8%	15%	15%
total	n	10	47	57
	avg	1.25	1.05	1.09
	CoV	13%	14%	15%

V_{test}/V_{sim}		with stirrups	without stirrups	total
90° ETS	n	6	24	30
	avg	1.18	1.01	1.04
	CoV	16%	12%	14%
45° ETS	n	4	23	27
	avg	1.33	1.14	1.17
	CoV	8%	13%	13%
total	n	10	47	57
	avg	1.24	1.07	1.10
	CoV	14%	14%	15%

Fig. 10 - Comparisons between experimental and predicted shear capacities of members with ETS steel reinforcing bars, according to a) CSA-S6 [37] for stirrups, b) the detailed design procedure , V_{det} , and c) the simplified design procedure, V_{sim}

In Fig. 10, in contrast to Table 1, the actual shear strength values for each specimen were used rather than the average values of n tests. The tables in Fig. 10 examine not only the overall accuracy of the prediction methods, but also the influence of stirrups and the influence ETS steel bar angle. The predicted strengths, V_{csa} , assuming that the members were strengthened with stirrups, result in a number of unconservative predictions. Although the V_{test}/V_{csa} has an average value (avg) of 1.00, it has a high coefficient of variation (CoV) of 20%. For the 4 members tested by Valerio [30] as well the members tested by Barros and Dalfré [31] and Breveglieri *et al.* [32], the anchorage length ℓ_a is practically deep enough to fully develop the bonded bars within d_v and the bonded shear reinforcement behaves similarly to stirrups. For these members, the proposed method predictions are close to the code predictions, which confirms the influence of the anchorage length, ℓ_a, on the bond behavior.

For the proposed methods, the shear capacities are generally accurately estimated. For the detailed and the simplified methods, the average test to predicted strengths are 1.09 and 1.10 and the CoV are 15% and 15%, respectively. The CSA, detailed and simplified methods give conservative predictions for the case when stirrups are present. The detailed and simplified methods give generally conservative strength predictions for all cases without stirrups, with slightly more conservative predictions for ETS steel bars at 45°.

Models that predict the shear capacity of steel ETS bars have been proposed by Breveglieri *et al.* [34], while other models examine the influence of FRP ETS [24, 42]. It is noted that there are significant differences in the models proposed by Breveglieri *et al.* [34] and the method described in this paper. Breveglieri *et al.* [34] developed an empirical model based on 19 tests, 3 of which failed in flexure-shear. He also developed a mechanical model that used the crack angle observed in his test results.

The model developed in this paper in based on the Modified Compression Field Theory together with accounting for the bond characteristics of the embedded bars. The results were validated with 57 specimens from the literature and the two methods proposed provide generally conservative predictions suitable for design.

7 CONCLUSIONS

Several authors have proposed using embedded-through-section steel reinforcing bars to increase the shear capacity. While this shear strengthening method can significantly increase the shear capacity, current shear design methods specified by codes were developed for anchored stirrups and can significantly overestimate the capacity of members with bonded shear reinforcement. The conclusions from this study apply to members strengthened with embedded-through-section (ETS) steel reinforcing bars.

In a member with ETS steel reinforcing bars, it appears that the bar stress at a crack and thus, the bonded bar shear capacity, is a function of the bar embedment and the crack width. The diagonal crack location determines the embedment of a bonded bar. A bonded bar with a small embedment may require a larger crack to develop their full capacity compared with stirrups that are well anchored. Moreover, they may fail by debonding before reaching their yield strength. Consequently, design methods have to be adjusted to account for the behavior of bonded bars.

The shear design method proposed in this paper is based on the modified compression field theory and considers the average bar capacity within the shear depth according to the bar development length to determine the shear contribution provided by the ETS steel reinforcing bars. That average bonded bar capacity must be considered to determine the minimum amount and the maximum spacing of bonded shear reinforcement. Also, large shear cracks may be expected in members with ETS steel reinforcing bars, thereby reducing the aggregate interlock. This effect is considered by determining a crack width increase in the RC member, which is used to reduce the concrete shear capacity. The detailed and simplified methods proposed in this paper result in very good shear capacity predictions for members strengthened with ETS steel reinforcing bars. These methods apply to members with different bars spacings and hence account for the contribution of partially developed and fully developed bonded bars.

ACKNOWLEDGMENTS

The authors wish to express their gratitude to the Natural Sciences and Engineering Research Council of Canada (NSERC, CREATE-INFRA), the “Fonds de Recherche du Québec – Nature et Technologies” (FRQNT), and the “Ministère des Transports” of Québec for financing this research work. The authors also acknowledge the contributions of the Research Center on Concrete Infrastructures (CRIB).

REFERENCES

[1] Collins MP, Kuchma D. How Safe Are Our Large, Lightly Reinforced Concrete Beams, Slabs, and Footings? ACI Structural Journal. 1999;96:482-90.

[2] Collins MP, Mitchell D. Prestressed Concrete Structures. Englewood Cliffs, NJ: Prentice-Hall; 1991.

[3] Elstner RC, Hognestad E. Laboratory Investigation of Rigid Frame Failure. ACI Journal. 1957;28:637-68.

[4] Aboutaha RS, Burns NH. Strengthening of Prestressed Concrete Composite Beams Using External Prestressed Stirrups. PCI Journal. 1994;39:64-74.

[5] Khalifa A, Gold WJ, Nanni A, Aziz A. Contribution of Externally Bonded FRP to Shear Capacity of RC Flexural Members. Journal of Composites for Construction. 1998;2:195-202.

[6] Khalifa A, De Lorenzis L, Nanni A. FRP Composites for Shear Strengthening of RC Beams. In: Humar J, Razaqpur AG, editors. The Third International Conference on Advanced Composite Materials in Bridges and Structures. Ottawa, ON: Canadian Society for Civil Engineering; 2000. p. 137-44.

[7] Nanni A, Di-Ludovico M, Parretti R. Shear Strengthening of a PC Bridge Girder with NSM CFRP Rectangular Bars. Advances in Structural Engineering. 2004;7:97-109.

[8] Adhikary BB, Mutsuyoshi H. Shear Strengthening of Reinforced Concrete Beams Using Various Techniques. Construction and Building Materials. 2006;20:366-73.

[9] Teng S, Kong F-K, Poh SP, Guan LW, Tan K-H. Performance of Strengthened Concrete Deep Beams Predamaged in Shear. ACI Structural Journal. 1996;93:159-71.

[10] Teng JG, Lam L, Chen JF. Shear Strengthening of RC Beams with FRP Composites. Progress in Structural Engineering and Materials. 2004;6:173-84.

[11] Teng JG, Chen GM, Chen JF, Rosenboom OA, Lam L. Behavior of RC Beams Shear Strengthened With Bonded or Unbonded FRP Wraps. Journal of Composites for Construction. 2009:394.

[12] Dias SJE, Barros JAO. Shear Strengthening of T Cross Section Reinforced Concrete Beams by Near-Surface Mounted Technique. Journal of Composites for Construction. 2008;12:300-11.

[13] Mofidi A, Chaallal O, Cheng L, Shao Y. Investigation of Near Surface Mounted Method for Shear Rehabilitation of Reinforced Concrete Beams Using Fiber Reinforced Polymer Composites. Journal of Composites for Construction. 2016;20:14.

[14] De Lorenzis L, Nanni A. Shear Strengthening of Reinforced Concrete Beams with Near-Surface Mounted Fiber-Reinforced Polymer Rods. ACI Structural Journal. 2001;98:60-8.

[15] Mofidi A, Chaallal O. Renforcement à l'effort tranchant des poutres en béton armé à l'aide de matériaux composites collés en surface : Avancées et perspectives pour la norme CSA-S806. Canadian Journal of Civil Engineering. 2011;38:556-69.

[16] Baghi H, Barros JAO. Design Approach to Determine Shear Capacity of Reinforced Concrete Beams Shear Strengthened with NSM Systems. ASCE Journal of Structural Engineering. 2017;143:04017061.

[17] Yungon Kim WMG, James OJ. Shear Design Considering Interaction between Steel Stirrups and Carbon Fiber-Reinforced Polymer Strips. ACI Structural Journal. 2017;114:803-14.

[18] Colalillo MA. Behaviour of Shear-Critical Reinforced Concrete Beams Retrofitted with Externally Applied Fibre-Reinforced Polymers [Thesis]. Toronto: University of Toronto; 2012.

[19] Colalillo MA, Sheikh SA. Behavior of Shear-Critical Reinforced Concrete Beams Strengthened with Fiber-Reinforced Polymer - Experimentation. ACI Structural Journal. 2014;111:1373-84.

[20] Colalillo MA, Sheikh SA. Behavior of Shear-Critical Reinforced Concrete Beams Strengthened with Fiber-Reinforced Polymer - Analytical Method. ACI Structural Journal. 2014;111:1385-96.

[21] Mofidi A, Chaallal O. Shear Strengthening of RC Beams with EB FRP: Influencing Factors and Conceptual Debonding Model. Journal of Composites for Construction. 2011;15:62-74.

[22] Qin S, Dirar S, Yang J, Chan AHC, Elshafie M. CFRP Shear Strengthening of Reinforced-Concrete T-Beams with Corroded Shear Links. Journal of Composites for Construction. 2015;19:04014081.

[23] Chaallal O, Mofidi A, Benmokrane B, Neale K. Embedded Through-Section FRP Rod Method for Shear Strengthening of RC Beams: Performance and Comparison with Existing Techniques. Journal of Composites for Construction. 2011;15:374-83.

[24] Mofidi A, Chaallal O, Benmokrane B, Neale K. Experimental Tests and Design Model for RC Beams Strengthened in Shear Using the Embedded Through-Section FRP Method. Journal of Composites for Construction. 2012;16:540-50.

[25] Fernández Ruiz M, Muttoni A, Kunz J. Strengthening of Flat Slabs Against Punching Shear Using Post-Installed Shear Reinforcement. ACI Structural Journal. 2010;107:434-42.

[26] Bédard F. Renforcement à l'effort tranchant des dalles de béton épaisses en condition de service [Thesis]. Québec, QC: Université Laval; 2018.

[27] Cusson B. Renforcement des dalles épaisses en cisaillement [Thesis]. Québec, Canada: Université Laval; 2012.

[28] Provencher P. Renforcement des dalles épaisses en cisaillement [Thesis]. Québec (QC): Université Laval; 2011.

[29] Fiset M, Bastien J, Mitchell D. Methods for Shear Strengthening of Thick Concrete Slabs. Journal of Performance of Constructed Facilities. 2017;31:10.

[30] Valerio P. Realistic shear assessment and novel strengthening of existing concrete bridges [Thesis]. Bath: University of Bath; 2009.

[31] Barros JAO, Dalfré GM. Assessment of the Effectiveness of the Embedded Through-Section Technique for the Shear Strengthening of Reinforced Concrete Beams. Strain. 2013;49:75-93.

[32] Breveglieri M, Aprile A, Barros JAO. Embedded Through-Section shear strengthening technique using steel and CFRP bars in RC beams of different percentage of existing stirrups. Composite Structures. 2015;126:101-13.

[33] Kunz J, Fernández Ruiz M, Muttoni A. Enhanced safety with post-installed shear reinforcement. fib Symposium. Tel-Aviv, Israel; 2013. p. 4.

[34] Breveglieri M, Aprile A, Barros JAO. RC beams strengthened in shear using the Embedded Through-Section technique: Experimental results and analytical formulation. Composites Part B. 2016;89:266-81.

[35] fib. fib Model Code for Concrete Structures 2010. fédération internationale du béton: Ernst and Sohn; 2013.

[36] CSA-A23.3. Design of Concrete Structures. Toronto, ON: Canadian Standards Association 2019. p. 301.

[37] CSA-S6. Canadian Highway Bridge Design Code. 12th ed. Toronto, ON: Canadian Standards Association; 2019. p. 1185.

[38] AASHTO. LRFD Bridge Design Specifications 9th Ed. . Washington DC: American Association of State Highway and Transportation Officials; 2020. p. 1912.

[39] Dias SJE, Barros JAO. Shear strengthening of RC T-section beams with low strength concrete using NSM CFRP laminates. Cement and Concrete Composites. 2011;33:334-45.

[40] Bousselham A, Chaallal O. Effect of transverse steel and shear span on the performance of RC beams strengthened in shear with CFRP. Composites Part B: Engineering. 2006;37:37-46.

[41] Grande E, Imbimbo M, Rasulo A. Effect of Transverse Steel on the Response of RC Beams Strengthened in Shear by FRP: Experimental Study. Journal of Composites for Construction. 2009;13:405-14.

[42] Valerio P, Ibell TJ, Darby AP. Deep embedment of FRP for concrete shear strengthening. Proceedings of the Institution of Civil Engineers - Structures and Buildings. 2009;162:311-21.

[43] Vecchio FJ, Collins MP. The Modified Compression-Field Theory for Reinforced-Concrete Elements Subjected to Shear. ACI Journal. 1986;83:219-31.

[44] Collins MP, Mitchell D, Adebar P, Vecchio FJ. A General Shear Design Method. ACI Structural Journal. 1996;93:36-60.

[45] Bentz EC, Collins MP. Development of the 2004 CSA A23.3 Shear Provisions for Reinforced Concrete. Canadian Journal of Civil Engineering. 2006;33:521-34.

[46] Appl J-J. Tragverhalten von Verbunddübeln unter Zugbelastung (Load bearing behaviour of bonded anchors under tension loading) [Thesis]. Stuttgart: Universität Stuttgart; 2009.

[47] Lowes LN, Moehle JP, Govindjee S. Concrete-Steel Bond Model for Use in Finite Element Modeling of Reinforced Concrete Structures. ACI Structural Journal. 2004;101:501-11.

[48] Meszaros J. Tragverhalten von Einzelverbunddübeln unter zentrischer Kurzzeitbelastung [Load bearing behavior of single bonded anchors under short-term centric loading]. Stuttgart: University of Stuttgart; 2002.

[49] Lettow S. Ein Verbundelement für nichtlineare Finite-Elemente-Analysen - Anwendung auf Übergreifungsstöße [Bond element for nonlinear finite element analysis - application to lap splices] [Thesis]. Stuttgart: University of Stuttgart; 2006.

[50] Villemure F-A, Fiset M, Bastien J, Mitchell D, Fournier B. Behavior of Bonded Bars Post-Installed in Concrete Affected by Alkali-Silica Reaction. ACI Materials Journal. 2019;116:179-91.

[51] Fiset M. Étude du comportement des éléments en béton armé post-renforcés à l'effort tranchant [Thesis]. Québec, QC: Université Laval; 2019.

[52] Mahrenholtz C. Seismic Bond Model for Concrete Reinforcement and the Application to Column-to-Foundation Connections [Thesis]. Stuttgart: Universität Stuttgart; 2012.

[53] Fiset M, Villemure F-A, Bastien J, Mitchell D. Behavior of Post-Installed Bonded Bars as Shear Reinforcement. ACI Structural Journal. 2020;117:159-68.

[54] Eligehausen R, Mallée R, Silva JF. Anchorage in Concrete Construction. Berlin, Germany: Ernst and Sohn; 2006.

[55] Fiset M, Bédard F, Bastien J, Mitchell D. Thick Concrete Slab Bridges: Study of Shear Strengthening. 10th International Conference on Short and Medium Span Bridges. Québec (QC): Canadian Society for Civil Engineering; 2018. p. 10.

[56] ACI-318. Building Code Requirements for Structural Concrete. Farmington Hills; 2019. p. 624.

[57] Hilti. North American Product Technical Guide : Anchor Fastening Technical Guide. 17 ed. Tulsa, OK; 2016.

[58] Fuchs W, Eligehausen R, Breen JE. Concrete Capacity Design (CCD) Approach for Fastening to Concrete. ACI Structural Journal. 1995;92.

[59] Eligehausen R, Blochwitz R, Fuchs W. Behavior and Design of Adhesive Anchors Under Sustained Load. ACI Special Publication 283 2012:1-14.

[60] ASTM-A996/A996M. Standard Specification for Rail-Steel and Axle-Steel Deformed Bars for Concrete Reinforcement. West Conshohocken, PA; 2016. p. 5.

[61] Fernández Ruiz M, Muttoni A, Gambarova PG. Analytical Modeling of the Pre- and Postyield Behavior of Bond in Reinforced Concrete. ASCE Journal of Structural Engineering. 2007;133:1364-72.

[62] Brantschen F. Influence of Bond and Anchorage Conditions of the Shear Reinforcement on the Punching Strength of RC Slabs [Thesis]. Lausanne: École Polytechnique Fédérale de Lausanne; 2016.

[63] Brantschen F, Faria DMV, Fernández Ruiz M, Muttoni A. Bond Behaviour of Straight, Hooked, U-Shaped and Headed Bars in Cracked Concrete. Structural Concrete. 2016;17:799-810.

[64] Jirsa JO, Marques JL. A Study of Hooked Bar Anchorages in Beam-Column Joints. University of Texas at Austin: Department of Civil Engineering; 1972. p. 92.

[65] Rahal KN, Collins MP. Background to the General Method of Shear Design in the 1994 CSA-A23.3 Standard. Canadian Journal of Civil Engineering. 1999;26:827-39.

[66] Vecchio FJ. Disturbed Stress Field Model for Reinforced Concrete: Formulation. ASCE Journal of Structural Engineering. 2000;126:1070-7.

[67] Marti P, Alvarez M, Kaufmann W, Sigrist V. Tension Chord Model for Structural Concrete. Structural Engineering International. 1998;8:287-98.

[68] Yoon YS, Cook WD, Mitchell D. Minimum Shear Reinforcement in Normal, Medium, and High-Strength Concrete Beams. ACI Structural Journal. 1996;93:576-84.

[69] Frosch RJ. Behavior of Large-Scale Reinforced Concrete Beams With Minimum Shear Reinforcement. ACI Structural Journal. 2000;97:814-20.

[70] ASCE-ACI-445. Recent Approaches to Shear Design of Structural Concrete. ASCE Journal of Structural Engineering. 1998;124:1375-417.

[71] Lubell AS, Bentz EC, Collins MP. Shear Reinforcement Spacing in Wide Members. ACI Structural Journal. 2009;106:205-14.

[72] Serna-Ros P, Femandez-Prada MA, Miguel-Sosa P, Debbt OAR. Influence of Stirrup Distribution and Support Width on shear Strength of Reinforced Concrete Wide Beams. Magazine of Concrete Research. 2002;54:181-91.

[73] Muttoni A, Fernández Ruiz M. Design Method for Post-Installed Shear Reinforcement with Hilti Tension Anchors HZA. Ecublens: HILTI-AG Fastening and Protection Systems; 2013. p. 12.

APPENDIX – NOTATION

The following symbols are used in the paper:

a = Shear span, distance between load and support

a_g = Maximum aggregate size

A_b = Area of a reinforcing bar

A_p = Area of a prestressed reinforcement

A_s = Area of longitudinal reinforcement on the flexural tension side of the member

A_v = Area of shear reinforcement within a distance s

b_w = Width of the web

C = Coefficient determining the minimum amount of shear reinforcement

d = Distance from the extreme compression fiber to centroid of tension reinforcement

d_a = Diameter of an anchorage plate

d_b = Diameter of a reinforcing bar

d_v = Effective shear depth, the greater of $0.9d$ and $0.72h$

E_p = Modulus of elasticity of prestressed reinforcement

E_s = Modulus of elasticity of non-prestressed reinforcement

f_b = Equivalent bond strength

f_{by} = Bond strength when $\ell = \ell_d$

f_{b0} = Basic bond strength

f'_c = Concrete compressive strength

f_{po} = Stress in the prestressed reinforcement

f_{scr} = Bar stress at a crack

f_y = Yield strength of reinforcement

h = Member height

k_0 = Initial stiffness of the bond-slip relationship

k_c = Concrete breakout capacity factor

k_d = Coefficient taking into account debonding of a reinforcing bar

k_{dg} = Aggregate size parameter

k_v = Maximum spacing ratio of vertical shear reinforcement

k_w = Ratio between the bar displacement at a crack and the crack width

ℓ = Total bar embedment

ℓ_{bar} = Total length of a bar

ℓ_a = Length of a bar exceeding the effective shear depth

ℓ_d = Development length of reinforcement

ℓ_t = Transition length of reinforcement

M_u = Moment at the section

n_p = Number of reinforcing bar extremities with a mechanical anchorage system

N_u = Axial load normal to the cross section of a member (positive in tension)

p_d = Proportion of the member affected by Δ_{wd}

p_t = Proportion of the member affected by Δ_{wt}

p_s = Proportion of the member affected by Δ_{ws}

α_0 = Simplified bond slip curve parameter

s = Longitudinal spacing of transverse reinforcement

s_{ze} = Equivalent crack spacing parameter

s_1 = Slip at the beginning of the bond strength plateau

s_2 = Slip at the end of the bond strength plateau

V_c = Shear attributed to the concrete

V_n = Nominal shear capacity

V_u = Shear at the section

V_s = Shear attributed to shear reinforcement

w = Crack width

w_{by} = Crack width at yielding of a bonded bar

w_{sy} = Crack width at yielding of stirrups

x_{cr} = Location of a crack

α = Angle between inclined shear reinforcement and longitudinal member axis

β = Factor accounting for shear resistance of cracked concrete

Δ_w = Crack width increase due to bond slip

Δ_{wd} = Crack width increase due to the behavior in the zone ZD

Δ_{wt} = Crack width increase due to the behavior in the zone ZT

Δ_{ws} = Crack width increase due to the behavior in the zone ZS

ε_1 = Principal tensile strain

ε_x = Longitudinal strain at mid-depth of a member (positive when tensile)

η = Efficiency of a bonded bar, ratio between average capacity and bar yield strength

Ω_θ = Factor considering the reduction of the concrete breakout capacity for inclined bars

θ = Angle between diagonal compression stress field and longitudinal member axis

ρ_s = Ratio of longitudinal tension reinforcement